where $\Phi(x)$ is the probability integral. We note that in case c) the mean depolarization rates are not equal in the longitudinal and transverse directions:

$$\langle \Lambda_\parallel^i(\theta,\ \alpha)\rangle = \langle \Lambda_\parallel^j(\theta,\ \alpha)\rangle = \langle \Lambda_\parallel^k(\theta,\ \alpha)\rangle = {}^6/_8\Lambda^0, \qquad (26)$$

$$\langle \Lambda_\perp^i(\theta,\ \alpha)\rangle = \langle \Lambda_\perp^j(\theta,\ \alpha)\rangle = \langle \Lambda_\perp^k(\theta,\ \alpha)\rangle = {}^5/_8\Lambda^0. \qquad (27)$$

6. It turns out thus that the muon method can, in principle, yield information on the degree of magnetic anisotropy of the chromium. If application of a magnetic field of given strength causes rotation of the magnetic moments, then the muon polarization damping in the polycrystal will depend on the direction of the external magnetic field relative to the initial muon momentum—longitudinal or transverse. At large values of the anisotropy, the average depolarization rate in a polycrystal should not depend strongly on the orientation of the external magnetic field relative to the initial polarization. This result can be explain in general form by the following arguments.

According to (9) and (11), the longitudinal and transverse depolarization rates are given by

$$\Lambda_\perp = G_{xx} + \frac{G_{yy}+G_{zz}}{2} = \frac{\Lambda^0}{2} + \frac{G_{xx}}{2}, \qquad (28)$$

$$\Lambda_\parallel = G_{yy} + G_{zz} = \Lambda^0 - G_{xx}, \qquad (29)$$

where $\Lambda^0 = \mathrm{Tr}\,G_{\alpha\beta}$. For the mean values we have

$$\langle \Lambda_\perp \rangle = \frac{\Lambda^0}{2} + \frac{\langle G_{xx}\rangle}{2}, \quad \langle \Lambda_\parallel \rangle = \Lambda^0 - \langle G_{xx}\rangle.$$

If $\langle \Lambda_\perp \rangle = \langle \Lambda_\parallel \rangle$, then $\langle G_{xx}\rangle = \Lambda^0/3$, meaning that in a poly-

crystal all the directions of the internal magnetic fields are on a par. If $\langle G_{xx}\rangle \langle \Lambda^0/3$, i.e., the internal magnetic fields at the muon (and hence also the magnetic moments) are directed predominantly in a plane perpendicular to the external magnetic field, then $\langle \Lambda_\parallel \rangle < \langle \Lambda_\perp \rangle$. On the other hand if $\langle G_{xx}\rangle > \Lambda^0/3$, i.e., the internal magnetic fields are directed predominantly along the external field, then we should have $\langle \Lambda_\parallel \rangle < \langle \Lambda_\perp \rangle$.

[1]W. J. Kossler, A. T. Fiory, D. E. Murnick, C. E. Stronach, and W. F. Lankford, Hyperfine interaction 3, 287 (1977).
[2]V. G. Grebinnik, I. I. Gurevich, V. A. Zhukrov, I. G. Ivanter, A. L. Klimov, A. P. Marych, E. V. Mel'nikov, B. A. Nikol'skiĭ, A. V. Pirogov, A. N. Ponomarev, V. I. Selivanov, V. A. Suetin, and S. V. Fomichev, Pis'ma Zh. Eksp. Teor. Fiz. 28, 456 (1978) [JETP Lett. 28, 423 (1978)].
[3]E. I. Kondorskiĭ, Zonnaya teoriya magnetizma (Band Theory of Magnetism), part II, Izd. MGU, Moscow, 1977.
[4]S. A. Werner, A. Arrott, and H. Kendrick, Phys. Rev. 155, 528 (1967).
[5]I. G. Ivanter and S. V. Fomichev, Teoriya depolyarizatsii μ^+-mezonov redkozemel'nykh metallakh vblizi tochek Neelya (Theory of Depolarization of mesons in Rare Earth Metals near the Neel Points), IAE-2999, Moskva, 1978.

Investigation of second-harmonic generation in diffused LiNbO₃ waveguides

E. M. Zolotov, V. M. Pelekhatyĭ, A. M. Prokhorov, and V. A. Chernykh

The conditions for efficient second-harmonic generation in diffused LiNbO₃ waveguides are considered. The overlap integrals of the interacting modes are computed as functions of the waveguide parameters. It is shown that the highest second-harmonic generation efficiency is attained in the case when the E_1 (1.06 μ) and H_2 (0.53 μ) modes interact. Second-harmonic generation is investigated experimentally in the 10^{-2}–10^3-W ($\lambda = 1.06\mu$) pump–power range, and a comparison with the calculations is carried out. The highest nonlinear-conversion efficiency is 16% for a peak pump power of 1 kW.

Integral optics opens up general possibilities for raising the effectiveness of nonlinear interactions. The use of optical waveguides allows us to obtain in a film of thickness of the order of the wavelength of high light intensities from relatively low-power sources, e.g., gas lasers. In contrast to the three-dimensional case, when the contraction of the luminous flux to small dimensions gives rise to its considerable diffraction divergence, in a waveguide the small cross section of

the flux (and, consequently, its high density) is preserved along its entire length. Another merit of thin-film waveguides is the possibility of obtaining in them phase matching of the interacting waves as a result of the dispersion of the modes. This allows the use of isotropic media possessing large nonlinear coefficients. As to anisotropic waveguides, they do not need temperature adjustment for obtaining ninety-degree phase matching. The latter is achieved by a proper choice of

the refractive-index profile.

However, in spite of the obvious advantages of the use of optical waveguides for nonlinear conversion, advances in this field have been quite modest. In particular, the second-harmonic generation realized in the various materials has been characterized by an efficiency 2–3 orders of magnitude lower than the theoretical estimates,[1-3] which is apparently explained by the low quality of the waveguides used. As is well known,[4] to achieve efficient nonlinear conversion, the nonuniformity of the film in thickness should not exceed 0.01 μ per 1 mm. The nonfulfillment of this condition leads to the destruction of the phase synchronism and, consequently, to the lowering of the intensity of the second harmonic. The use by Uesugi and Kimura[5] of a diffused waveguide in $LiNbO_3$ for nonlinear conversion allowed continuous-wave ($\lambda = 0.53$ μ) second-harmonic generation with an efficiency that agreed in order of magnitude with the theoretical estimate ($\approx 0.01\%$). In this case, however, the sample was cooled to a temperature below 0 °C, which naturally complicated the apparatus. Earlier we had achieved second-harmonic generation without temperature adjustment with a conversion efficiency $\approx 0.01\%$[6] and $\approx 16\%$[7] under conditions of pumping respectively by a continuous-wave and a pulsed garnet laser.

In the present paper we carry out a theoretical and an experimental analysis of the possibilities of realizing efficient second-harmonic generation in diffused optical $LiNbO_3$ waveguides in a wide range of pump powers. The analysis is carried out for pumping at the wavelength $\lambda = 1.06$ μ.

PHASE MATCHING IN AN OPTICAL WAVEGUIDE

As is well known, for efficient second-harmonic generation it is necessary to achieve phase matching of the interacting waves. In anisotropic crystals the compensation of the dispersion at the frequencies of the fundamental and second harmonics is achieved through the use of differently polarized interacting waves. The direction of phase matching in this case coincides with the direction of intersection of the indicatrices of their refractive indices $n(\varphi_0, \omega) = n(\varphi_0, 2\omega)$, a direction which in the three-dimensional case is determined by the birefringence and dispersive power of the crystal. If the direction of synchronism does not coincide with any of the crystallophyiscal axes, then the interaction range will be limited by the divergence of the fundamental- and second-harmonic waves as a result of double refraction. Therefore, to realize an effective nonlinear interaction, it is preferable to use ninety-degree synchronism, which forbids double refraction, and which is realized in the three-dimensional case by means of temperature adjustment.

The refractive indices are higher in the optical waveguides than in the substrate. If their increments Δn^0 and Δn^e exceed the dispersion $n_\omega - n_{2\omega}$ of the refractive indices at the fundamental- and second-harmonic frequencies, then a compensation for $n_\omega - n_{2\omega}$ can be obtained on account of the dispersion of the modes. In this case isotropic media can well be used. In the case

of "weak" waveguides, i.e., when the increment in the refractive index of the waveguide layer is much smaller than the refractive index of the substrate ($\Delta n \ll n_2$), phase matching is achieved (as in the three-dimensional case) only because of double refraction, but the use of mode dispersion allows a significant broadening of the phase-matching region.

It is not difficult to verify this by examining Fig. 1, which shows in outline the regions of possible location of the indicatrices of the modes at the fundamental- and second-harmonic frequencies in an anisotropic waveguide with a negative crystal as the substrate. The regions in which the indicatrices of modes of ordinary and extraordinary polarizations can lie are hatched, and their overlap defines the region where phase matching is possible. For each pair of modes phase matching occurs at a definite angle, to wit, at the angle at which the indicatrices of the modes intersect. By varying the depth, the shape of the profile, or the increment in the refractive index of the waveguide, we can vary the phase-matching angles for the modes selected for the nonlinear interaction. It should be noted that, in order to be able to effect this type of variations, it is necessary to know well the dependence of the phase characteristics of the waveguide on its structure parameters and also know how to control the latter during the fabrication of the waveguides. For titanium-diffused waveguides in $LiNbO_3$ the angles at which phase matching of the modes is possible lie within the limits $\varphi \approx 75-90°$, i.e., by suitably choosing the waveguide parameters we can realize ninety-degree phase matching without recourse to temperature adjustment.

OVERLAP OF THE INTERACTING-MODE FIELDS

The realization of phase matching (even ninety-degree phase matching) in an optical waveguide is not a sufficient condition for obtaining efficient nonlinear conversion. The decisive role is played by the degree of overlap of the optical fields of the interacting modes, the degree of overlap being characterized by the overlap integral:

$$I = \left(\int_{-\infty}^{0} Y_\omega{}^2(y) Y_{2\omega}(y)\,dy \right)^2 \Big/ \left(\int_{-\infty}^{0} Y_\omega{}^2(y)\,dy \right)^2 \left(\int_{-\infty}^{0} Y_{2\omega}{}^2(y)\,dy \right), \quad (1)$$

where $Y_\omega(y)$ and $Y_{2\omega}(y)$ are the transverse distributions of the mode fields at the fundamental and second-harmonic frequencies. The overlap integral (for an overlap obtained for the phase-matching case in the plane-wave
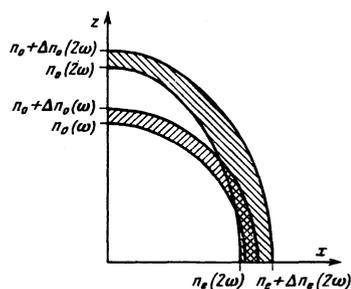
FIG. 1. Regions where the indicatrices of modes of ordinary and extraordinary polarizations in $LiNbO_3$ can lie.

approximation[8,9]) enters into the expression for the second-harmonic-generation efficiency:

$$\eta = \frac{P_{2\omega}}{P_p} = \text{th}^2\left(\frac{8\pi^2 d}{\lambda n}\left(\frac{8\pi P_p I}{cnW}\right)^{1/2} L\right) \quad (2)$$

where d is the nonlinearity coefficient, P_p is the pump power, $P_{2\omega}$ is the second-harmonic power, L is the interaction range, λ is the pump wavelength, n is the refractive index of the material, and W is the beam width in the plane of the waveguide.

As can be seen from the expression (1), the overlap integral depends on the field distribution of the modes of the two harmonics, which are quite difficult to determine for diffused waveguides, since their profiles are not known a priori; even if they are known, an analytical solution to the wave equation for them does not always exist. If LiNbO$_3$ is used, then the situation is further complicated by the fact that this anisotropic crystal and the waveguides in them have different profiles for ordinary and extraordinary polarizations. Furthermore, in Ti-diffused waveguides in LiNbO$_3$ the waveguide is formed not only as the result of the diffusion of Ti into the crystal, but also as the result of the back diffusion of Li$_2$O. The two processes are described by different kinetics; therefore, the profile of the waveguide for extraordinary polarization turns out to be complicated.[10]

In the present paper we determine $Y_\omega(y)$ and $Y_{2\omega}(y)$ by a previously developed[10,11] method, which allows the determination of the characteristics (including the mode fields and dispersion dependences) of diffused waveguides with any refractive-index distribution profile. This method is based on the approximation of the sought waveguide profile by functions allowing the analytic solution of the wave equation. In Ti-diffused waveguides in (Y-cut) LiNbO$_3$, for ordinary polarization of the waves, the transverse-distribution profile $n_0(y)$ is determined by a combination consisting of a parabola and an exponential function smoothly joined together:

$$n_0(y) = \begin{cases} n_1 + \Delta n(1 - y^2/a^2), & -c \leqslant y \leqslant 0, \\ n_1 + \Delta n(1 - c^2/a^2)e^{(y+c)/h}, & -\infty < y < -c, \end{cases}$$

where a and h are respectively parameters of the parabola and the exponential function, while c is the coordinate of the point where the functions are matched.

The waveguide profile for extraordinary waves is, as has already been noted, more complicated, and is determined by a nonsmooth combination of a parabola, shifted in the direction of the upper medium, and an exponential function:

$$n_e(y) = \begin{cases} n_1 + \Delta n\dfrac{1-(y+b)^2/a^2}{1-b^2/a^2}, & -c-b \leqslant y \leqslant 0, \\ n_1 + \Delta n\dfrac{1-c^2/a^2}{1-b^2/a^2}\exp\left(\dfrac{y+c+b}{h}\right), & -\infty < y < -c. \end{cases}$$

Here b is a parameter characterizing the displacement of the parabola toward the upper medium.

The mode fields in the indicated waveguides are obtained from the solution of the wave equation for the ordinary waves (E-polarization), and have the form

$$Y(y) = \begin{cases} C_1 \eta e^{-\eta^2/2}{}_1F_1(^3/_4 - s_m/4, \, ^3/_2, \, \eta^2), & -c \leqslant y \leqslant 0, \\ C_2 J_{\nu_m}(\alpha e^{\xi/\alpha}), & -\infty < y < -c, \end{cases}$$

where $_1F_1$ is a confluent hypergeometric function, $J_{\nu m}(\alpha, \xi)$ is a Bessel function,

$$\bar{a} = (2n_1\Delta n)^{1/2}ka, \quad \eta = \bar{a}^{1/2}y/a,$$
$$\gamma_m = (n_m{}^* - n_1)/\Delta n, \quad s_m = \bar{a}(1-\gamma_m),$$
$$\xi = (2n_1\Delta n(1-c^2/a^2))^{1/2}k(y+c), \quad \alpha = \bar{a}\frac{a}{c}(1-c^2/a^2)^{1/2},$$
$$\nu_m = \bar{a}(a/c - c/a)\gamma_m^{1/2}.$$

For the extraordinary waves (H-polarization)

$$Y(y) = [C_1\eta_1 F_1(^3/_4 - s_m/4, \, ^3/_2, \, \eta^2)$$
$$+ C_2\,{}_1F_1(^1/_4 - s_m/4, \, ^1/_2, \, \eta^2)]e^{-\eta^2/2}, \quad -c-b \leqslant y \leqslant 0,$$
$$Y(y) = C_3 J_{\nu_m}(\alpha e^{\xi/\alpha}), \quad -\infty < y < -c-b.$$

Here

$$\bar{a} = \left(\frac{2n_1\Delta n}{1-b^2/a^2}\right)^{1/2}ka, \quad \eta = \bar{a}^{1/2}\frac{y+b}{a},$$
$$s_m = (1-\gamma_m(1-b^2/a^2)), \quad \nu_m = 2(2n_1\Delta n\gamma)^{1/2}kh,$$
$$\xi = \left(2n_1\Delta n\frac{1-c^2/a^2}{1-b^2/a^2}\right)^{1/2}k(y+b+c), \quad \alpha = 2\left(2n_1\Delta n\frac{1-c^2/a^2}{1-b^2/a^2}\right)^{1/2}kh.$$

The constants C_1, C_2, and C_3 are determined from the condition that the wave function should vanish at the boundary with air and be continuous at the matching point.

Using the obtained mode-field distributions in a Ti-diffused waveguide in LiNbO$_3$, we computed their overlap integrals I_{1m} ($m = 1, 2, 3, 4$) for the interaction $o + o = e$. Figure 2 plots shows of I_{1m} as a function of the dimensionless thickness $\alpha = (2n_1^0\Delta n^0)^{1/2}ka^0$ for typical parameters of the Ti-diffused waveguide.[10] In the calculations carried out we did not take into consideration the insignificant variations of the structure-parameter ratios c/a and h/a as α is varied, since they had practically no effect on the nature of the dependences of the overlap integrals $I_{1m}(\alpha)$. We do not present here the results of the investigation of the overlap integrals I_{nm} of the modes in thicker waveguides ($\alpha > 6$), where $n > 1$, since phase matching in such waveguides are attainable only for higher modes ($m \gtrsim 3$), and therefore the overlap integrals are small.

The analysis performed shows that, for the optimization of second-harmonic generation in Ti-diffused waveguides from the standpoint of the overlap integral for the interacting modes, it is necessary to choose
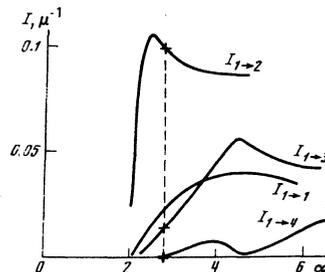
FIG. 2. Dependence of the overlap integrals for different interactions on the dimensionless waveguide thickness α (the vertical dashed line corresponds to the thickness of the invertigated sample).

waveguides of small thickness ($\alpha \approx 3$) with the use of lower-mode interactions.

EXPERIMENTAL INVESTIGATIONS AND ANALYSIS OF THE RESULTS

For the realization and investigation of second-harmonic generation, we used a waveguide prepared by means of thermal diffusion of Ti into a Y-cut LiNbO$_3$ crystal during six hours at 960 °C. The mode spectrum (n_m^*) of the waveguide was determined with the aid of a goniometer by the method of extracting the radiation through a photoconductive grid ($\Lambda = 0.3462\ \mu$) deposited on a surface.[11] The appropriate diffusion regime was chosen on the basis of the results of the above-performed analysis; the obtained waveguide was polished a little with a view to optimizing the thickness. There were excited in it the modes $H_1 - H_4$, E_1 and E_2 at the wavelength $\lambda = 0.53\ \mu$ and the modes E_1 and H_1 at the wavelength $\lambda = 1.06\ \mu$. Figure 4 shows the indicatrices of the refractive indices for the modes of the obtained waveguide at the fundamental- and second-harmonic frequencies. It can be seen from the figure that the conditions for phase matching are fulfilled only for the following $o + o = e$ type interactions:

$$E_1(1.06) \rightarrow H_2(0.53);$$
$$E_1(1.06) \rightarrow H_3(0.53),$$
$$E_1(1.06) \rightarrow H_4(0.53).$$

The indicatrix of the H_1 mode does not intersect the indicatrices of the fundamental modes; therefore, it is impossible to obtain phase matching for H_1.

On the basis of the n_m^* spectra obtained for the waveguide in question, we found the refractive-index distribution profiles for ordinary and extraordinary polarizations. These profiles were characterized by the following parameters:

$$n_1^o = 2.2335; \quad \Delta n^o = 0.0035;$$
$$a^o = 4\ \mu\ ; \quad (c/a)^o = 0.7;$$
$$h^o = 1.5\ \mu\ ;$$

$$n_2^* = 2.2308; \quad \Delta n^* = 0.015; \quad a^* = 14\ \mu\ ; \quad (c/a)^* = 0.97;$$
$$(b/a)^* = -0.63; \quad h^* = 8.5\ \mu\ ;$$

With the aid of the obtained profiles we computed the mode fields of the waveguide in question (Fig. 3) and de-
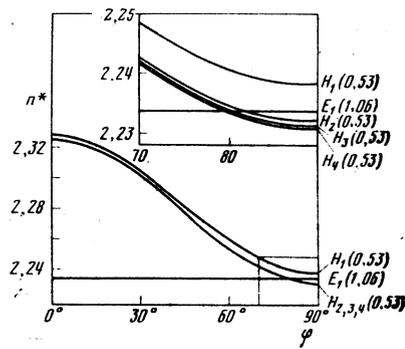
FIG. 4. The indicatrices of the effective refractive indices for the modes of the investigated diffused waveguide.

termined the overlap integrals I_{1m} ($m = 2, 3, 4$). The integral I_{12} was the largest, and was close to the optimum value (see Fig. 2); therefore, we used the $E_1(1.06) \rightarrow H_2(0.53)$ conversion. The pumping was performed by Nd^{3+}:YAG lasers operating in the continuous and pulsed regimes. The radiation was introduced (and led out) with the aid of a rutile prism in the phase-matching direction; the beam width in the waveguide was $\approx 100\ \mu$. The pumping by the cw laser was realized within the limits $2 - 13$ mW (according to the power that could be fed into the waveguide), and the highest conversion efficiency was 8×10^{-5}. In the case of pumping by the pulsed laser in the free-generation regime (50–300 mW), the fundamental- and second-harmonic pulses (of duration $\approx 10^{-4}$ sec) were observed on an oscillograph screen, which allowed us to determine their peak powers and the corresponding conversion-efficiency values with allowance for the temporal shape. In the case of pumping by the pulsed laser in the Q-switched regime ($\Delta t \approx 10^{-8}$ sec), the pulses had roughly the shape of a Gaussian function, and their durations at the wavelengths of the fundamental and second harmonics differed by a factor of $\sqrt{2}$, a fact which was taken into account in the computation of the conversion efficiency.

The dependence, obtained upon processing the experimental data, of the second harmonic generation efficiency on the pump power is shown in Fig. 5. The highest conversion efficiency was obtained for a pump power ≈ 1 kW, and was equal to 16%. For the purpose of
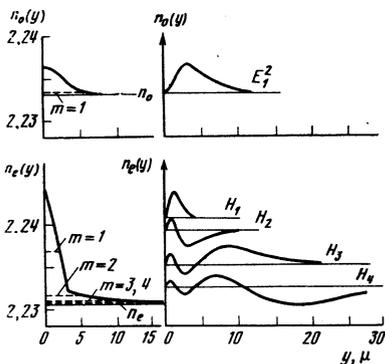
FIG. 3. Refractive-index and optical-field distributions for the ordinary (a) and extraordinary (b) waves of the investigated diffused waveguide: a) $\lambda = 1.06\ \mu$; b) $\lambda = 0.53\ \mu$.
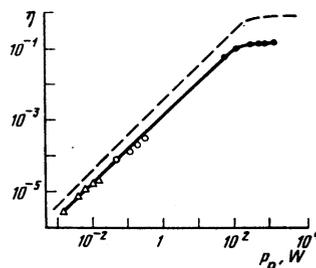
FIG. 5. Theoretical (dashed line) and experimental (solid line) pump-power dependences of the second-harmonic-generation efficiency (the experimental points correspond to pumping by a cw laser ($\triangle$), a pulsed laser operating in the free-generation regime ($\bigcirc$), and a pulsed laser operating in the Q-switched regime ($\bullet$)).

comparing the theory with experiment, we computed the dependence of the conversion efficiency on the pump power with the aid of the formula (2) for plane waves. The length of the path along which the E_ω^1 and $H_{2\omega}^2$ modes interacted was $L \approx 8$ mm, but since the synchronism was not a ninety-degree one, in the expression (2) the quantity L was replaced by the product $(LL_0)^{1/2}$, where L_0 is the aperture length ($L_0 \approx 4$ mm). The overlap integral $I_{12} = 0.1 \ \mu^{-1}$, while the nonlinear-interaction coefficient $d = d_{13} = 1.3 \times 10^{-8}$ esu.[12] The divergence of the radiation in the plane of the waveguide was neglected in the computations, since its magnitude ($\approx 10'$) was smaller than the angular phase-matching width (see Fig. 6). We also neglected the attenuation of the surface wave, in view of its weakness (<1 dB/cm).

The computed pump-power dependence of the nonlinear conversion efficiency (see Fig. 5) turned out to be appreciably raised with respect to the experimental dependence, which has a limiting value already at values of $\eta = 16\%$. This discrepancy is explained, first, by the nonuniformity of the investigated waveguide in thickness ($\Delta a \approx 0.1 \ \mu$), a nonuniformity which appeared as a result of the polishing of the surface after the Ti diffusion (this effect is confirmed by the broadening of the n_m^*-spectrum lines); second, by the refractive-index discontinuities, induced by the light of the second harmonic, and observed at pump powers ≈ 1 kW. Thus, the nonlinear-conversion efficiency can be increased further by improving the quality of the surface of the waveguide, as well as by raising the threshold for the appearance of optical inhomogeneities.

We also investigated the dependence of the second-harmonic power on the angle between the direction of propagation of the pumping wave and the optical axis of the crystal (Fig. 6). It can be seen from the figure that this curve has an asymmetric character with respect to the central peak ($E_1 \to H_2$ interaction). This is explained by the fact that the peaks corresponding to the $E_1 \to H_3$ and $E_1 \to H_4$ interactions are superimposed on the left wing of the curve. The relative heights of the peaks are in satisfactory agreement with the values of the overlap integrals. The width of the central peak exceeded the corresponding theoretical value by a factor of four, which is also explained by the inhomogeneity, of the waveguide.

Thus, the above-presented method of computing the profiles of a waveguide and the transverse fields of the modes allowed us to determine the optimal parameters of a diffused waveguide in LiNbO$_3$ for second-harmonic generation and to fabricate a waveguide in which efficient second-harmonic generation has been realized at pump powers several orders of magnitude lower than
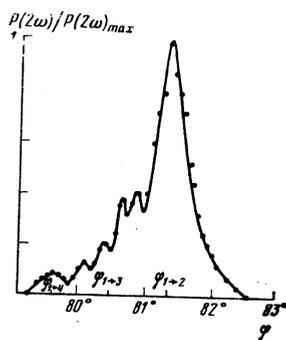
FIG. 6. Angular dependence of the second-harmonic power.

in the three-dimensional analogs. The possibility exists of raising further the effectiveness of the nonlinear interaction.

[1] H. Ito, N. Uesugi, and H. Inaba, Appl. Phys. Lett. 25, 385 (1974).

[2] A. T. Reutov and P. P. Tarashchenko, Opt. Spektrosk. 37, 786 (1974) [Opt. Spectrosc. (USSR) 37, 447 (1974)].

[3] J. P. van der Ziel, R. M. Mikuljak, and A. Y. Cho, Appl. Phys. Lett. 27, 71 (1975).

[4] J. T. Boyd, IEEE J. Quantum Electron. QE-8, 788 (1972).

[5] N. Uesugi and T. Kimura, Appl. Phys. Lett. 29, 572 (1976).

[6] E. M. Zolotov, V. G. Mikhalevich, V. M. Pelekhatyi, A. M. Prokhorov, V. A. Chernykh, and E. A. Shcherbakov, Pis'ma Zh. Tekh. Fiz. 4, 219 (1978) [Sov. Tech. Phys. Lett. 4, 108 (1978)].

[7] E. M. Zolotov, V. M. Pelekhatyi, A. M. Prokhorov, and V. A. Chernykh, Tezisy dokladov IX Vsesoyuznoi konferentsii po kogerentnoi i nelineinoi optike (Abstracts of Papers Presented at the Ninth All-Union Conference on Coherent and Nonlinear Optics), Leningrad, June 1978.

[8] F. Zernike and J. Midwinter, Applied Nonlinear Optics, Wiley-Interscience, New York, 1973 (Russ. Transl., Mir, 1976).

[9] E. M. Conwell, IEEE J. Quantum Electron. QE-9, 867 (1973).

[10] E. M. Zolotov, V. M. Pelekhatyi, A. M. Prokhorov, S. A. Semiletov, and E. A. Shcherbakov, Pis'ma Zh. Tekh. Fiz. 3, 241 (1977) [Sov. Tech. Phys. Lett. 3, 95 (1977)].

[11] E. M. Zolotov, V. A. Kiselev, A. M. Prokhorov, and E. A. Shcherbakov, Kvantovaya Elektron. (Moscow) 3, 1672 [Sov. J. Quantum Electron. 6, 905 (1976)].

[12] D. N. Nikogosyan, Kvantovaya Elektron. (Moscow) 4, 5 (1977) [Sov. J. Quantum Electron. 7, 1 (1977)].

Translated by A. K. Agyei